Journal of Plant Physiology **163** (2006) 996–1007

Available online at www.sciencedirect.com

ScienceDirect

JOURNAL OF
PLANT PHYSIOLOGY

www.elsevier.de/jplph

Acoustic emission analysis and experiments with physical model systems reveal a peculiar nature of the xylem tension

Ralf Laschimke[a,*], Maria Burger[a], Hartmut Vallen[b]

[a]*Zollern GmbH, Hitzkofer Str. 1, D-72488 Sigmaringen, Germany*
[b]*Vallen Systeme GmbH, Schäftlarner Weg 26, D-82075 Icking, Germany*

Received 27 February 2006; accepted 10 May 2006

KEYWORDS
Acoustic emissions;
Cohesion theory;
Gas bubbles;
Peristaltic transport;
Xylem transport

Summary

Advanced acoustic emission analysis, special microscopic examinations and experiments with physical model systems give reasons for the assumption that the tension in the water conducting system of vascular plants is caused by countless minute gas bubbles strongly adhering to the hydrophobic lignin domains of the xylem vessel walls. We ascertained these bubbles for several species of temperate deciduous trees and conifers. It is our hypothesis that the coherent bubble system of the xylem conduits operates as a force-transmitting medium that is capable of transporting water in traveling peristaltic waves. By virtue of the high elasticity of the gas bubbles, the hydro-pneumatic bubble system is capable of cyclic storing and releasing of energy. We consider the abrupt regrouping of the wall adherent bubble system to be the origin of acoustic emissions from plants. For *Ulmus glabra*, we recorded violent acoustic activity during both transpiration and re-hydration. The frequency spectrum and the waveforms of the detected acoustic emissions contradict traditional assumptions according to which acoustic emissions are caused by cavitation disruption of the stressed water column. We consider negative pressure in terms of the cohesion theory to be mimicked by the tension of the wall adherent bubble system.

Abbreviations: A, surface area; AE, acoustic emissions; AAE, audible acoustic emissions; CLSM, confocal laser scanning microscopy; *E*, total energy; *F*, gravitational force; *n*, moles; *p*, pressure; *s*, translation; *S*, entropy; *V*, volume; *T*, temperature; UAE, ultrasonic acoustic emissions; ε modulus of elasticity; μ, chemical potential; σ, surface tension; τ, three-dimensional distortion.

*Corresponding author. Schlosshalde 1, D-72479 Strassberg, Germany. Tel.: +49 7434 8288; fax: +49 7434 315 908.
E-mail address: Laschimke@t-online.de (R. Laschimke).

0176-1617/$ - see front matter © 2006 Elsevier GmbH. All rights reserved.
doi:10.1016/j.jplph.2006.05.004

Introduction

The predominantly passive character of long-distance water transport has frequently been questioned. However, it has been repeatedly demonstrated, even in context of acoustic emissions (Borghetti et al., 1991), that the application of poisons as metabolic inhibitors to the water transport system has little or no effect on water movement, reinforcing the concept that non-living cells are primarily involved in water transport and no essential input of metabolic energy takes place. Despite this, various suggestions of active pumping have been proposed time and again, but no mechanical or biochemical devices that could achieve such pumping have been found. Also, the frequently cited root pressure would not be capable of transporting water to the tops of tall trees. In sum, the idea of the cohesion theory that water ascends in the apoplast part of the xylem, largely under the direct influence of the evaporation from the leaves, is most likely the correct explanation, but the transmission of pulling forces through the water column is still puzzling.

Milburn and Johnson (1966) reported that transpiring plants generate acoustic emissions in the audio frequency range. Since that time, Milburn's findings have been considered proof of the validity of the cohesion theory, according to which the ascent of sap is caused by a gradient of negative pressure. The cohesion theory has been repeatedly questioned from a physical point of view because the claimed metastability of water under negative pressure has not been demonstrated for air saturated water. However, the soil water taken up by the roots is air saturated. Despite this inconsistency, challengers of the cohesion theory are usually rejected with reference to the acoustic emissions discovered by Milburn. Seen in the light of the cohesion theory, the acoustic emissions are caused by cavitation-disruptions of the water column under negative pressure. This argument was weakened when Tyree and Dixon (1983) introduced the ultrasonic frequency range into the investigations. It has now become clear that the AAE is only the tip of the iceberg. The overabundance of the UAE turned out to be a problem. Presupposing that each acoustic event is attributable to a cavitation event, it appears impossible to place the countless cavitation defects within the limited number of water conducting conduits. The problem is compounded since the cavitation-defects are supposed to be instantly embolized by air, and therefore the affected vessel tubes malfunction. Several assumptions of incessant embolism repair have been made recently by Zwieniecki and Holbrook (2000). However, a demonstrable repair mechanism has not been found to date.

Simultaneous monitoring of AAE and UAE by Ritman and Milburn (1990) revealed a significant time pattern of the acoustic emissions with leading UAE for intense transpiration and rising AAE for declining transpiration. Unfortunately, these authors eliminated the acoustic emissions during the nightly re-hydration phase. Apparently, the AE-signals of the re-hydration phase could not be explained within the context of cohesion theory. Milburn (1993) suggested that the mysterious UAE be ignored, and considered the AAE to be the most reliable indicator of cavitation. In a previous investigation, we argued that the acoustic emissions from plants are not caused by cavitation under negative pressure, but by sudden surface rearrangements of groups of wall adherent microbubbles under positive pressure (Laschimke, 1989). The existence of gas bubbles in the xylem conduits has been known for years. It is generally known that gas bubbles, which fill the whole lumen of the vessels, form so-called Jamin chains. The Jamin chains do not contribute to the driving forces of water transport; rather, they are barriers. The discovered wall adherent microbubbles, however, are much smaller in diameter than the vessels tubes. Such bubbles are largely stable and do not immediately result in embolism. When we presented the first micrographs in 1989, the microbubbles seemed to be an absurdity, seen in the light of the governing cohesion theory. On the other hand, Zimmermann and co-workers regarded the wall adherent microbubbles as an attractive concept of water transport by Marangoni-forces (Zimmermann et al., 1993). Marangoni flow requires a permanent concentration gradient in the transported water. This gradient has been taken for granted by Zimmermann, but no evidence could be provided up to now. Because Marangoni flow scarcely generates acoustic emissions, Zimmermann took into consideration several other acoustic origins, such as aspirating pits, occurrence of flow turbulence, fusion of gas bubbles adhering to the walls, cracks in the cell walls under strain, drying out of the bark, shrinking of the stem diameter and xylem bending (Zimmermann et al., 2004). Aiming to shed more light on the mysterious acoustic emissions from plants, we applied advanced methods of event detection and AE-analysis. By means of a special arrangement of the acoustic sensors, we were able to eliminate some of the named dubious origins of AE signals. In order to substantiate the results of our acoustic emission testing, we furthered our investigations with special microscopic examinations and experiments with physical model systems.

Materials and methods

Acoustic emissions

We selected a 4-year-old potted *Ulmus glabra* for examination. The broad leaves of *Ulmus glabra* facilitate the linkage of the special sensors we used in our investigation. Usually, acoustic sensors are linked to partly de-barked living stems or branches. We placed the sensors directly on the upper surface of living leaves as shown in Fig. 1b. This unusual arrangement allows monitoring of acoustic events right next to the place of transpiration. The transpiration of the investigated leaf was suffered practically no interference because the majority of the transpiring stomata are located on the untouched underside of the leaf. To record transpiration data simultaneously with acoustic data, we fitted the potted young elm tree to a computerized electronic scale as shown in Fig. 1a. To avoid uncontrolled evaporation, we covered the flowerpot with a polyethylene foil. The young elm was well watered before data acquisition. The temperature in the laboratory was constant at 22 °C and a relative humidity of 60%. Thus, the transpiration depended primarily on the intensity of the sunlight and the rhythm of day and night. Our experiments were carried out from the middle of July to the middle of August 1998.

We used the mass-loaded piezoelectric sensor SE-45 from Dunegan Engineering (USA), which exhibits optimum response in the range between 20 and 120 kHz. Experience has shown that, in the frequently used MHz range, the density of the acoustic emissions is extremely high. For the enormous number of the MHz signals, the storage of the waveforms of the individual signals is practically impossible, unlike the range of 20–120 kHz, where the signals are within reasonable limits. The threshold of signal detection was 26 dB, which corresponds to 20 μV at the sensor output. By means of a controlling sensor that was not in contact with the leaf surface, we discriminated and eliminated background noise from the relevant acoustic data. To obtain maximum information, we employed the Vallen system AMSY4 equipped with transient recorders, which store the complete waveforms of a maximum of 5000 signals.

Microscopic examination

Encouraged by the results of our acoustic emission testing, we decided to attempt to confirm our previous findings of microbubbles adhering at the lignin domains of the xylem vessel walls. Lignin can be detected by its yellow-green auto-fluorescence when excited by blue light. In a normal epifluorescence microscope, the intensity of the lignin fluorescence is low and in general, the source of the fluorescence cannot be localized sharply due to the stray light and the low depth of focus. This disadvantage is overcome by confocal laser scanning microscopy (Laschimke, 1991). The finer points of the surface structure of the vessel walls were made visible by means of SEM. The nonuniform wetting behavior of the xylem vessel walls were made visible by means of water immersion microscopy; a living branch of our young *Ulmus glabra* was bent down into a container of tap water with the temperature of the branch. Then a sample with a length of about 3 cm was cut off, and a tangential cut was made. Then the sample that remained immersed in water was transferred under the microscope equipped with high-resolution lenses for water immersion (numerical aperture 1.25). This procedure lasted only a few minutes.

Physical model systems

The special properties of wall adherent bubbles are evident through experiments with model systems. Although our experimental devices do

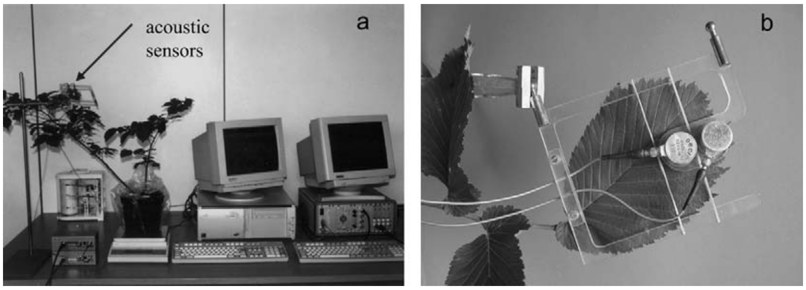

Figure 1. Simultaneous detection of acoustic emissions and transpiration loss: (a) experimental set-up and (b) leaves of *Ulmus glabra* with measuring sensor (left) and controlling sensor (right).

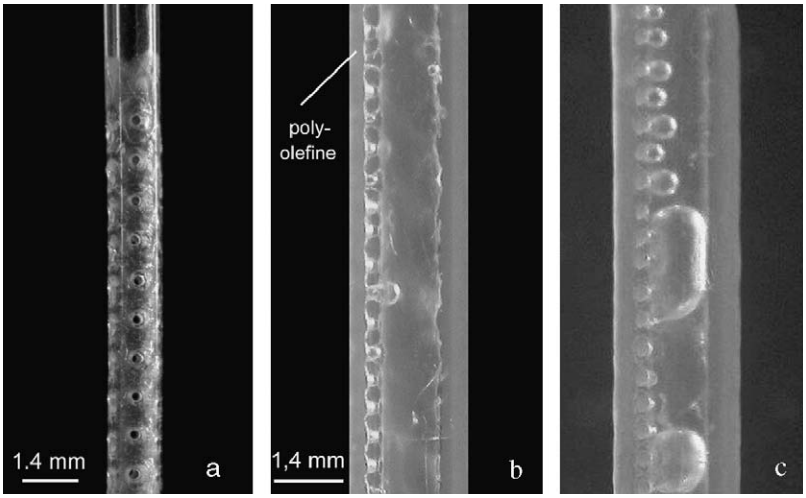

Figure 2. Experiments with a glass capillary perforated by a laser beam: (a) 40 symmetrically arranged lateral holes; (b) 13 lateral holes in one row, sheathed with hydrophobic polyolefine. Formation of gas bubbles at the hydrophobic bottoms of the lateral blind holes after 2 h; and (c) the gas bubbles according to (b) after 5 h. Embolism due to formation of Jamin chains.

not accurately simulate the structural features of xylem vessels, these devices demonstrate impressively the physical behavior of wall adherent gas bubbles. Fig. 2a shows a glass capillary perforated by means of a laser beam. We sheathed the perforated section with transparent hydrophobic polyolefin and immersed the prepared capillary tube into air-saturated water. Shortly after immersion, air bubbles develop at the hydrophobic bottoms of the lateral blind holes. We then withdrew the capillary tube half out of the water container and compared the water column with that of a normal capillary tube. Fig. 3 shows that, by virtue of the lateral bubbles, the water column is held on a significantly higher level compared to a normal capillary tube. After some hours, the capillary tube became embolized by expanding bubbles and the formation of Jamin chains (Fig. 2b and c). It became obvious that lasting stability of the water column requires a much larger number of much smaller hydrophobic blind holes, similar to the xylem vessels walls, where the geometrical parameters have been optimized by nature. Consequently, we made efforts to miniaturize the perforations of the tube wall. This turned out to be unrealistic, but we were successful in preparing improved experimental devices with plane surfaces. Fig. 4 shows an array of densely arranged hydrophobic blind holes, each with a diameter of 0.05 mm. Related to the vessel pits of *Ulmus glabra*, even the miniaturized blind holes are still in the ratio of 50:1. The disadvantage of our miniaturized devices is that the peculiar shape of the wall adherent bubbles is not clearly visible

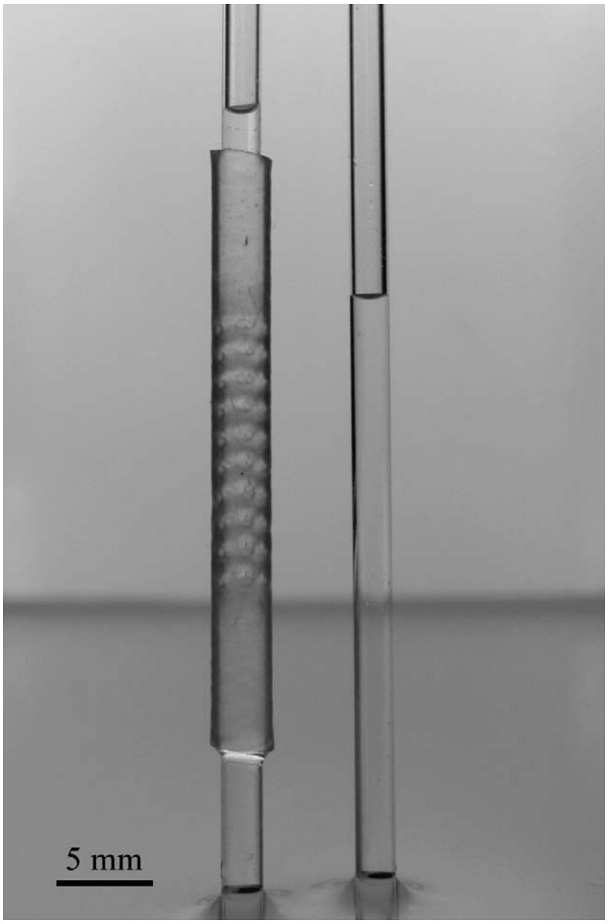

Figure 3. Capillary with 40 hydrophobic lateral blind holes and gas accumulations after 4 h. By virtue of the bubbles a longer continuous water column is held against gravity, compared to a normal capillary (right).

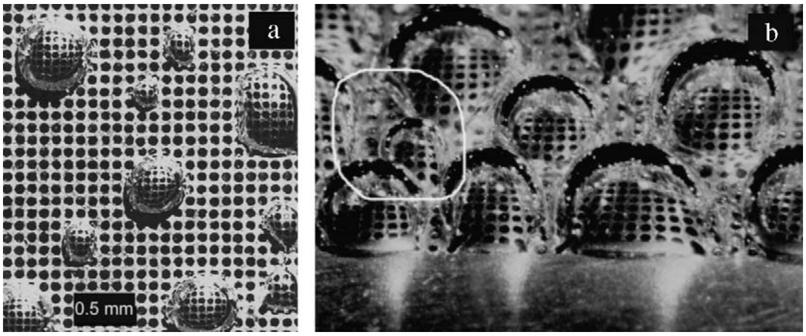

Figure 4. Array of numerous hydrophobic blind holes at a hydrophilic plane surface: (a) flat-shaped bubbles with undulated rims indicate mechanical tension between the solid base and the bubbles; and (b) two bubbles (marked area) at the moment of coalescence. The blurred contours indicate violent vibration.

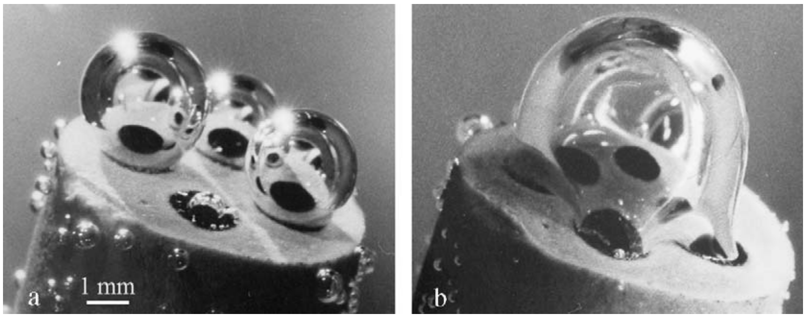

Figure 5. Formation of gas bubbles at four hydrophobic blind holes on a hydrophilic base: (a) initial stage; formation of spherical bubbles and (b) coalescence of spherical bubbles, formation of a multi-feet non-spherical bubble.

after their coalescence. Therefore, we made a model illustrated in Fig. 5, which allows observation of the modifications of these bubbles.

Results

Acoustic emissions

Figure 6a shows the transpiration loss for a testing period of 77 h. The regular course of the daily transpiration loss and the nightly refilling indicates normal hydration of the elm. To improve the assessment, we calculated the derivative curve called "transpiration intensity versus time", which reveals minimum transpiration intensity at night of about 15% of the maximum intensity during daylight (Fig. 6b). The diagram shows that acoustic emissions take place incessantly during both transpiration, and re-hydration. To differentiate the acoustic activity, we selected three types of acoustic events by the dominant AE-signal frequency, which is the frequency where the spectrum exhibits the maximum magnitude. Fig. 6c shows the correlation between acoustic activity and transpiration intensity in the three selected frequency ranges. We selected these special frequency ranges because the analysis of the AE signals in these frequency ranges turned out to be more conclusive than in other frequency ranges. The emissions in the lowest frequency range rise when the transpiration is rising. When the transpiration declines, the emissions in the lowest frequency range stop, and the emissions in the next higher frequency range start. The emissions in the highest frequency range weaken during maximum transpiration. The time pattern of the acoustic activity of the leaves of the investigated *Ulmus glabra* contradict the idea that acoustic emissions from plants occur in conjunction with intense transpiration. It is obvious that the acoustic activity also remains undiminished during the night refilling phase. The finer points of the different frequency pattern during transpiration and re-filling cannot be explained with the current level of data acquisition. Further investigations are necessary.

To approach the mechanism of acoustic emission generation, we analyzed the waveforms of the 2200 events, which are compiled in diagram Fig. 6. The review of the waveforms revealed great variability of amplitude, duration and frequency. The majority of the waveforms conflict with

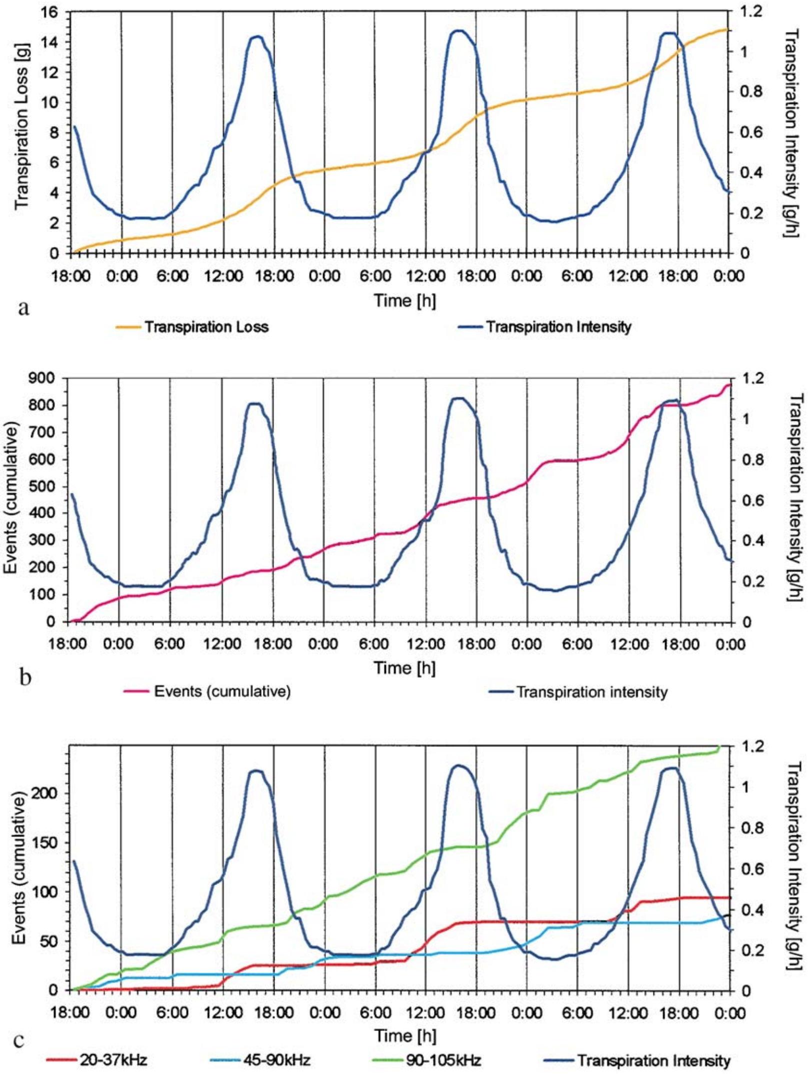

Figure 6. Correlation between transpiration and acoustic activity of *Ulmus glabra*: (a) transpiration loss and transpiration intensity versus time; (b) correlation between transpiration intensity and cumulative acoustic events; and (c) correlation between transpiration intensity and dominant frequencies.

cavitation-disruptions of the water column. After cavitation-disruption, the end of the broken water column should be violently retracted along the affected vessel tube, accompanied by a fast fading acoustic signal. We found this type of waveform only by a very limited number of signals (Fig. 7a). For the most part, the waveforms indicate lasting oscillation of the acoustic origins, as shown in Fig. 7b and c. This finding is not explicable in the context of cavitation-disruption.

Microscopic examinations

Figure 8 shows a SEM image of apoplast xylem vessel walls of *Ulmus glabra*. We noted fields of pits with wide-open apertures and fields of pits with narrow apertures and pit chambers. We assume different function in water transport for the different types of vessel pits, as explained in the "Discussion" section, below. For closer investigation, we prepared the pit chambers as in Fig. 9a. The SEM image and the corresponding CLSM image reveal ring-shaped lignin concentrations at the bottom of the pit chambers.

Figure 10 shows water immersion micrographs of the vessel walls of *Ulmus glabra* and *Quercus robur* at the end of May. Gas bubbles are clinging to the apertures of the vessel pits. Under special illumination conditions, the bubbles show total reflection, which is evidence of a liquid/gas interface. Prior to foliation of the leaves, the pit chambers are only partly filled with gas as visible in Fig. 11a and b. After foliation, bubbles balloon at the pit apertures,

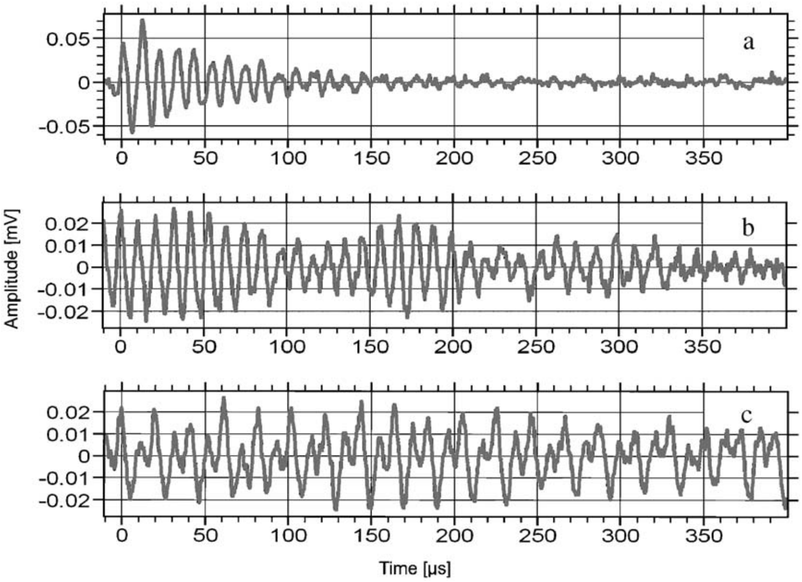

Figure 7. Typical variations of the waveforms of acoustic emissions from *Ulmus glabra*: (a) waveform monitored at irregular intervals both, during transpiration and refilling. This waveform indicates abrupt disruption of the water column. (b) Predominant waveforms during both transpiration and refilling, indicating vibration of the acoustic origin. (c) Frequently detected waveform, indicating overlapping of two vibrating acoustic origins.

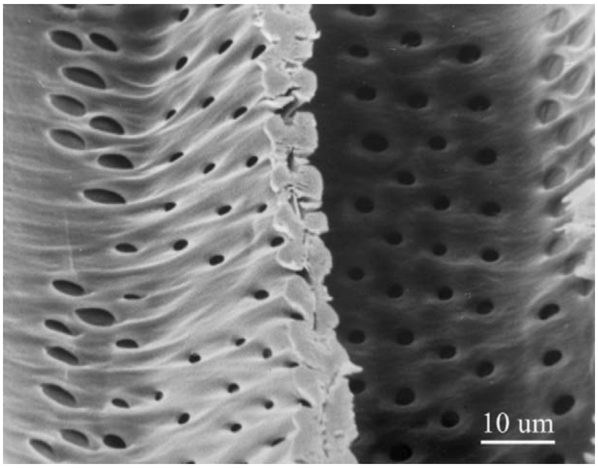

Figure 8. Xylem vessel walls of *Ulmus glabra*. The SEM image shows fields of wide-open pits and pits with narrow apertures and pit chambers.

as illustrated in Fig. 11c. When the expanding bubbles come into mutual contact they coalesce in flat bubble aggregates as shown in Fig. 11d. We realize that the observed bubbles are not exactly the same shape as in the intact vessel tubes, because the opening of the vessel tubes instantly causes a change of the hydraulic tension. However, spontaneous formation of new bubbles is inconceivable. We observed similar gas accumulations also at the xylem vessel walls of many other species. Figure 12 shows gas bubbles at the scalariform structured vessel walls of *Vitis vinifera* and in the tracheids of *Pinus silvestris*.

Physical model systems

Figure 5 shows an arrangement of four sizable hydrophobic blind holes at a hydrophilic base. When immersed in air-saturated water, spherical bubbles balloon at the blind holes. If the individual bubbles come into mutual contact, they coalesce into non-spherical bubbles. The deformed non-spherical bubbles are coupled to the solid by several stretched feet like a polyp. Obviously, the buoyancy alone cannot detach such multi-feet-bubbles, but a higher energy threshold must be surpassed. We consider the deformed multi-feet-bubble as being in a potential well. A potential well is a region surrounding a local minimum of all involved potential energy forms as explained in the "Discussion" (see below). Also, the gas bubbles at the vessel pits we consider to be fixed in potential wells. As visible in Fig. 4b, we were successful in creating a snapshot of bubbles at the moment of coalescence. The blurred contours of the coalescing bubbles are an indication of vibration. By virtue of the large vibration amplitude of the comparatively sizeable bubbles, the vibration after coalescence was detectable by photograph. Some of the emerged bubble configurations cover up to 30 blind holes. The undulated rims of the bubble

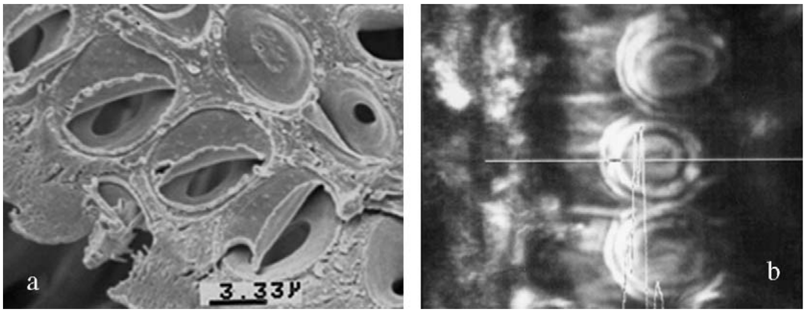

Figure 9. Lignin concentrations at the bottom of the pit chambers of *Ulmus glabra*: (a) SEM image and (b) CLSM image; fluorescence mode; extended focus. The white line shows the lignin concentration along the horizontal line.

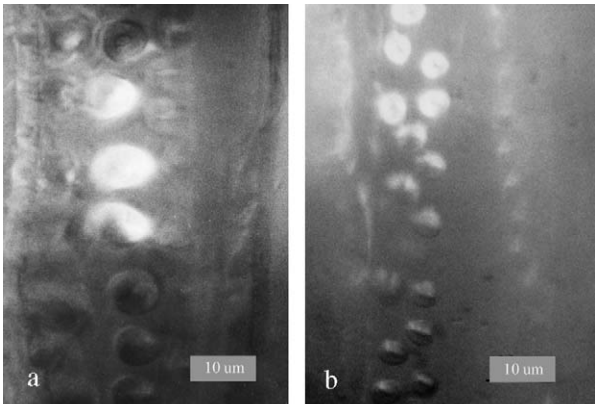

Figure 10. Gas bubbles at the apertures of the vessel pits of water conducting xylem vessel tubes in end of May. Water immersion micrographs: (a) *Ulmus glabra* and (b) *Quercus robur.*

configurations (Fig. 4a) indicate considerable distortion or tension between the bubbles and the solid.

Discussion

The existence of wall adherent gas bubbles at the walls of the operating xylem conduits cannot be reconciled with negative pressure in terms of the cohesion theory. We put forward a concept of passive water transport based on transpiration-induced pulling forces but exclusive of negative pressure.

The German forest botanist Hartig (1878) reported that 30 temperate angiosperm and gymnosperm tree species show significant high water content in January/February. Similar results were later reported by Lundegardh (1954), Gibbs (1958), and Glavac et al. (1990). The famous promoter of the cohesion theory Zimmermann (1983) conceded that the cohesion theory fails to explain the high water content of deciduous trees in winter. It has been speculated that the static hold of the water column results from the perfect wettability of the xylem vessel walls. However, it has been ignored that a resting Newtonian liquid like water does not create resultant forces in a direction tangential to the wetted wall. The same is true for osmotic forces. Only the forces of menisci might be capable of holding a continuous water column above the normal capillary height. This problem was debated by botanists 100 years ago, but extra menisci could not be found in the water transporting system. We want to emphasize that the discovered wall adherent microbubbles are nothing but hidden menisci.

On comparison of Fig. 11a and c, the question arises: what is the origin of the gas that causes the gradual expansion of the bubbles from April to May as visible in these figures? Most likely, the gas is CO_2 that develops in the spring by dissimilation of polysaccharides. The dissolved CO_2 diffuses together with the mobilized saccharides from the symplast part of the xylem into the water column of the apoplast conduits. When the transpiration starts, expansion of the wall adherent bubbles next to the site of transpiration takes place. However, excessive expansion of any individual bubble is avoided due to its cohesive interaction with neighboring bubbles. Instead of the local expansion of single bubbles, the expansion of the whole bubble layer propagates gradually in basal direction. In parallel, the solid structure of the vessel walls and the adjacent parenchyma cells becomes elastically distorted by interfacial forces according to our model system shown in Fig. 4a. Consequently, the water conducting system becomes charged with both surface energy and mechanical energy. In this phase, water is not taken up by the roots, but the water in the conduits becomes displaced in an apical direction. When the peristalsis-like expansion of the bubble system arrives at the roots, the hydro-pneumatic system is able to

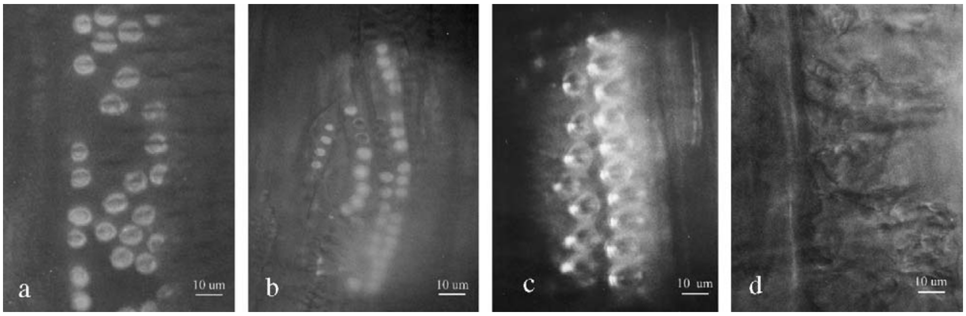

Figure 11. Gas accumulations at the xylem vessel walls in different stages of expansion. Water immersion micrographs: (a) *Ulmus glabra*, middle of April; (b) *Quercus robur*, middle of April; (c) *Ulmus glabra*, middle of May; and (d) *Ulmus glabra*, end of June.

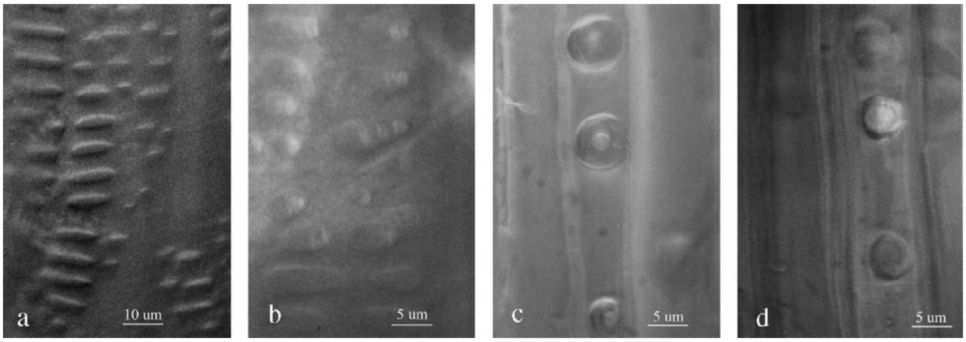

Figure 12. Gas accumulations at xylem vessel walls. Water immersion micrographs: (a) and (b) *Vitis vinifera*, end of May; and (c) and (d) *Pinus silvestis*, end of May.

take up water by release of stored energy. From now on, peristalsis-like drag flow takes place in apical direction. The drag flow develops because a Newtonian liquid is forced from the surface of a body, when the body is moved through the liquid. The propagating variation of the surface of the bubble system is equivalent to a moved body. In hydrodynamics, the component of the force in the direction of the moved body is called the drag. The component perpendicular to this direction is called the lift. In a narrow capillary tube, such as a xylem vessel tube, the lift superimposes in the center of the tube. Thus, the water column will be moved in direction of the drag as outlined in Fig. 13. This type of flow could be described as inverse Hagen–Poiseuille flow. Recent investigations by Zholkevich (2001) ascertained, for *Phaseolus vulgaris*, peristaltic water transport in a 1-min rhythm. Zholkevich postulated a metabolic corresponding regulatory and signal system that controls any still unknown mechanism of peristaltic water transport. We suggest regulation by stomata-controlled transpiration according to Fig. 13. Thürmer et al. (1999) ascertained that height-varying tension gradients developed in the vessels by variations in light intensity for the liana *Tetrastigma voinierianum*. To our knowledge, there are not any comprehensive data available from the literature for peristaltic water movement in trees. However, periodical changes in stem diameters of transpiring trees are well known.

It has long been recognized that plants can show rapid systemic response to localized stimuli, as reported by Malone and Alarcon (1995). For *Triticum*, an increase in leaf thickness up to 100% was measured, caused by scorch wounding of a neighboring leaf. Malone suggested that the transmitted signals are hydraulic in nature, but not compatible with other known models of signaling. The rate of propagation of the hydraulic signals measured by Malone is tens of $\mathrm{cm\,s^{-1}}$. From our point of view, the rapid swelling of the leaves can be explained only by rapid expansion of gas spaces, such as wall adherent bubbles. It is possible that the expansion of the gas spaces propagates from bubble to bubble by means of a domino effect.

A minimal temperature difference between moved air and leaves is enough for transpiration-induced transformation of heat into mechanical work of water transport. Every long-term energy transformation of heat into work requires a working cycle. Amazingly, in the cohesion theory, there has been claimed continuous passive water transport but any underlying working cycle is missing. We

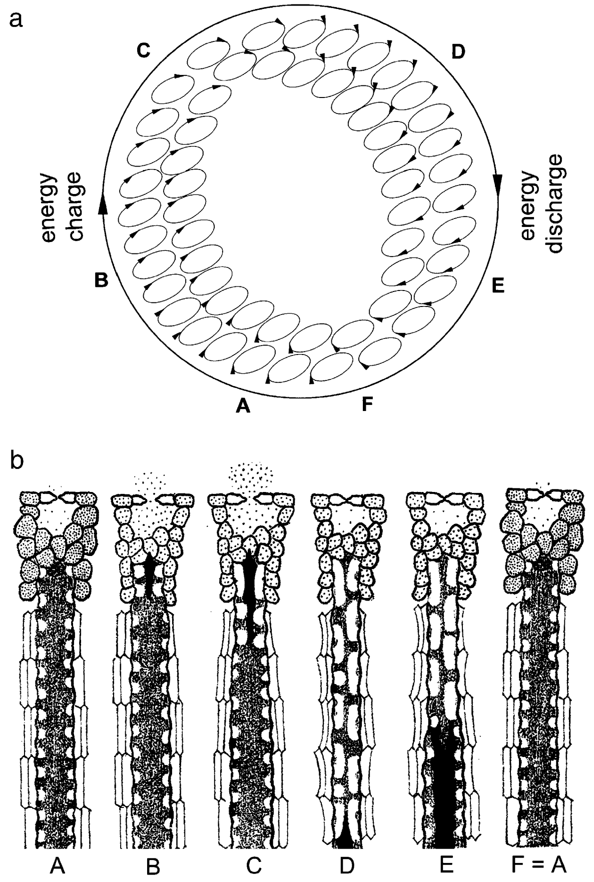

Figure 13. Transpiration-induced working cycle of xylem water transport: (a) total working cycle dismantled to many interlocked little working cycles and (b) phases of peristalsis-like water transport. (A) Full hydration. (B) Beginning of transpiration; gradual expansion of the wall adherent bubble system; displacement of water to the site of transpiration. (C) Intense transpiration, propagation of the expansion of the wall adherent bubble system; displacement of water to the site of transpiration; elastic distortion of the adjacent parenchyma; charge of mechanical energy. (D) Charge of energy complete; transpiration stop; basal uptake of water; discharge of energy; beginning of drag flow (dark marked) in apical direction. (E) Propagating discharge of mechanical energy; re-hydration by propagating drag flow of water in apical direction. (F) Full hydration.

suggest a working cycle according to Fig. 13a and b. We outlined this working cycle in a very simplified way, because, in our opinion, the formulation of a thermodynamic state equation seems to be nearly impossible. The concerned energy forms, however, can be easily expressed by the following Gibbs-equation:

$$dE = T\,dS + F\,ds - p\,dV + \sigma\,dA + \varepsilon\,dt + \Sigma\mu_i\,dn_i$$

where dE is the total energy; TdS thermal energy; Fds gravitational energy; $-p$dV compression energy; σdA surface energy; εdτ energy of the elastic distortion; $\Sigma\mu_i$dn_i chemical energy of the different chemical components. The interaction of the numerous energy forms corroborates the 'Multi-Force' Theory by Zimmermann et al. (2004).

The proposed working cycle starts after diffusion of sufficient gas into the permanently existing gas spaces of the pit chambers. Rising xylem tension corresponds with increasing size of the wall adherent bubbles. The working cycle breaks down after accumulation of a critical mass of gas, as outlined in Fig. 14. Every working cycle can be dismantled to interlocked little working cycles. In diagram Fig. 13a, the interlocked working cycles are not in phase. These differences of phase are consistent with our assumption that long distance water transport resembles peristaltic movements.

The hydration status is usually assessed by means of the water potential, which is the free energy of the water column associated with water per unit volume. To be precise, the water potential is a function of the solute potential, the pressure potential and the potential due to gravity. These terms in J m^{-3} are equivalent to pressure units such as Pascals (N m^{-2}). In our concept, additional energy terms are implicated: the surface energy of the bubble system σdA and the energy of the elastic distortion of the solid structure εdτ. These two terms are not associated with water per unit volume. The surface energy is partly associated with water molecules, but not with water per unit volume. The elastic energy is associated with the molecular structure of the solid. The term $-p$dV is mainly associated with the volume of gas contained

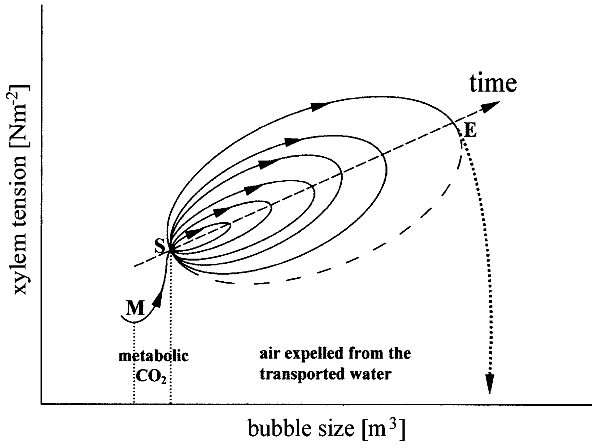

Figure 14. Local working cycle, according to Fig. 13. The gradual displacement of S along the time axis is unconsidered in this diagram. M minimum of free energy or potential well. S starting point of cyclic transformation of thermal energy into mechanical work. E embolism after excessive accumulation of gas.

in the wall adherent bubbles. There is hardly any free energy associated with the liquid phase under either positive or negative pressure. In consideration of this, we suggest redefining a "xylem potential", which includes the customary water potential, the gas potential of the bubble system, the surface potential of the bubble system and the elasticity potential of the solid structure.

The cohesive attraction between the individual bubbles enables the hydro-pneumatic system transporting surface energy in many small quantities from bubble to bubble. The gradually propagating expansion of the surface area of the whole bubble system represents, in fact, a flow of energy in the basal direction. It is our statement that this transport of non-metabolic energy from the leaves to the roots is the most important precondition of long-distance water transport in plants (Laschimke, 1990). In the last analysis, the water transporting system of plants can be viewed as an energy oscillator. To initiate the energy oscillation, the system must be deflected from the minimum of free energy or the potential well. This deflection requires an input of metabolic energy as outlined in Fig. 14. After foliation and at the beginning of transpiration, further input of metabolic energy is not necessary, provided that the transpiration-induced input of thermal energy is enough to compensate the friction loss of the water movement. It is clear that long-distance water transport requires lateral passages. Such passages are provided by the large number of pits with wide-open apertures (Fig. 8), which are free of gas accumulations and thus capable of transporting water through the cell wall perforations.

The hydration state of plant material can be assessed by both direct and indirect measuring methods. The indirect measuring pressure chamber test is based on the idea that negative pressure remains preserved in a detached sample, such as a twig. The preservation of negative pressure has been concluded from the retraction of the menisci of the cut water column into the cut xylem conduits. There is no denying that this retraction results from contractive forces in the water conducting system. However, tension cannot be preserved in the water column itself. From our point of view, the testing pressure in the pressure chamber primarily compresses the expanded wall adherent bubble system. The direct measurement of the xylem tension by the pressure probe test is based on self-acting intake of water into the xylem conduits. There is no doubt that this attraction of liquid is an indication of contractive forces in the water conducting system. However, in our view, the contractive forces are not caused by a gradient of negative pressure in the water column. In our opinion, the contractive forces result from the stressed hydro-pneumatic bubble system. That means we presume that negative pressure in terms of the cohesion theory is mimicked by the contractive forces of the wall adherent bubbles system.

The fragmentation of the water column cannot be prevented even in our transport model. Air dissolved in the transported water diffuses incessantly into the wall adherent bubbles. This way, embolism and dysfunction of the conduits is programmed as explained by Fig. 14. However, the dysfunction takes place after of a long period of problem-free water transport. To establish our findings, much more work is necessary. However, we hope that other investigators will critically evaluate our conclusions even in the present form.

References

Borghetti M, Edwards WRN, Grace J, Jarvis PG, Raschi A. The refilling of embolized xylem in *Pinus sylvestris*. Plant Cell Environ 1991;14:357–69.

Gibbs RD. Pattern in the seasonal water content of trees. In: Thimann KV, editor. The physiology of forest trees. New York: Ronald; 1958. p. 43–69.

Glavac V, Konies H, Ebben U. Auswirkung sommerlicher Trockenheit auf die Splintholz-Wassergehalte im Stammkörper der Buche (*Fagus sylvatica* L.). Holz Roh Werkst 1990;48:437–41.

Hartig, Th., 1878. Anatomie und Physiologie der Holzpflanzen, Berlin.

Laschimke R. Investigation of the wetting behaviour of natural lignin – a contribution to the cohesion theory of water transport in plants. Thermochim Acta 1989;151:35–56.

Laschimke R. Die Kohäsionstheorie des Wasserferntransportes. Allg Forst Z 1990;36:993–7.

Laschimke R. Localisation of lignin in wood by fluorescence confocal laser scanning microscopy. Mitt Bundesforschungsanst Forst Holzwirtsch 1991;68:243–8.

Lundegardh H. Transport of water in wood. Ark Bot 1954;3:89–119.

Malone M, Alarcon JJ. Only xylem-borne factors can account for systemic wound signalling in the tomato plant. Planta 1995;196:740–6.

Milburn JA. Cavitation. A review: past, resent and future. In: Water transport in plants under climatic stress. Cambridge: Cambridge University Press; 1993. p. 14–26.

Milburn JA, Johnson RPC. The conduction of sap. Detection of vibrations produced by sap cavitation in Rhicinus xylem. Planta 1966;69:43–52.

Ritman KT, Milburn JA. Monitoring of ultrasonic and audible emissions from plants with or without vessels. J Exp Bot 1990;42:123–30.

Thürmer F, Zhu JJ, Gierlinger N, Schneider H, Benkert R, Geßener P, et al. Diurnal changes in xylem pressure and mesophyll cell turgor pressure of the liana *Tetrastigma voinierianum*: the role of cell turgor in long-distance water transport. Protoplasma 1999;206: 152–62.

Tyree MT, Dixon MA. Cavitation events in *Tuja occidentalis*? Ultrasonic acoustic emissions from the sapwood can be measured. Plant Physiol 1983;72:1094–9.

Zholkevich VN. Water transport in plants and its endogenous regulation. Moscow: Nauka; 2001 (in Russian).

Zimmermann MH. Xylem structure and the ascent of sap. New York: Springer; 1983.

Zimmermann U, Haase A, Langbein D, Meinzer F. Mechanism of long distance water transport in plants: a re-examination of some paradigms in the light of new evidence. Philos Trans R Soc London 1993;B341: 19–31.

Zimmermann U, Schneider H, Wegner LA, Haase A. Water ascent in tall trees: does evolution of land plants rely on a high metastable state? New Phytol 2004;162: 575–615.

Zwieniecki MA, Holbrook NM. Bordered pit structure and vessel wall surface properties. Implications for embolism repair. Plant Physiol 2000;123:1015–20.